Uğur Çalıgülü
Halil Dikbaş
Mustafa Taşkın
Firat University
ucaligulu@firat.edu.tr
Elazig-Turkey

THE EFFECTS OF HIGH WELDINGS SPEED ON MICROSTRUCTURE AND MECHANICAL PROPERTIES OF DISSIMILAR COMPONENTS (AISI 430–AISI 304) WELDED BY CO_2 LASER BEAM WELDING

ABSTRACT
In this study, the effects of high welding speed on microstructure and mechanical properties of dissimilar welded components (AISI 430 ferritic stainless steel and AISI 304 austenitic stainless steel) by CO_2 laser beam welding was carried out. Laser beam welding experiments were carried out under argon and helium atmospheres at 2250 W constant heat input and 100-200-300 cm/min. welding speeds. The microstructures of the welded joints and the heat affected zones (HAZ) were examined by optical microscopy, SEM, EDS and X-Ray analysis. The tensile strength of the welded joints was measured. The result of this study indicated that; the width of welding zone became much thinner depending on the increased welding speed. Tensile strength values also confirmed this result. The best properties were observed at the specimens welded under helium atmosphere with a welding speed of 100 cm/min.
Keywords: Dissimilar Components (AISI 430-304), CO_2 Laser Beam Welding, Welding Speed, Microstructure, Mechanical Property

CO_2 LAZER IŞIN KAYNAĞI İLE BİRLEŞTİRİLEN FARKLI MALZEMELERİN (AISI 430-AISI 304) MİKROYAPI VE MEKANİK ÖZELLİKLERİNE YÜKSEK İLERLEME HIZININ ETKİSİ

ÖZET
Bu çalışmada, CO_2 lazer ışın kaynağı ile kaynak edilen farklı malzemelerin(AISI 430-AISI 304) mikroyapı ve mekanik özelliklerine yüksek ilerleme hızının etkisi incelenmiştir. Lazer kaynakları, argon ve helyum koruyucu gaz atmosferlerinde, 2250 W sabit kaynak gücünde ve 100-200-300 cm/dk ilerleme hızlarında yapılmıştır. Kaynak sonrası birleşme ara yüzeyinde ve ısının tesiri altında kalan bölgede(ITAB) meydana gelen mikroyapı değişiklikleri optik mikroskop, SEM, EDS ve X-Ray analizleri ile incelenmiştir. Malzemenin birleşme mukavemetini belirlemek için çekme deneyi yapılmıştır. Yapılan incelemeler sonrasında bütün kaynaklarda, artan ilerleme hızına paralel olarak kaynak bölgesinin genişliğinin azaldığı tespit edilmiştir. Çekme testleri de bu sonucu doğrulamaktadır. Helyum atmosferi altında ve 100 cm/dk ilerleme hızı uygulanarak yapılan lazer kaynağının, metalurjik ve mekanik açıdan kaynak kalitesi en yüksek birleştirme olduğu tespit edilmiştir.
Anahtar Kelimeler: Farklı Malzemeler (AISI 430-304), CO_2 Lazer Işın Kaynağı, Kaynak Hızı, Mikroyapı, Mekanik Özellikler

1. INTRODUCTION (GİRİŞ)

Ferritic stainless steels are widely used due to the fact that their corrosion resistance is higher at room temperature and they are much cheaper than the other stainless steels. Ferritic stainless steels contain 16-30% Cr within their structures in respect of addition of the alloying elements. This type of the steel can be formed easily and resist atmospheric corrosion well and thanks to these characteristics, it has a wide range of application in architecture, interior and exterior decoration, kitchen utensils, manufacturing of wash boilers and drying machines, food industry, automotive industry, and petrochemical and chemical industries [1, 2, 3, 4, and 5].

Austenitic-stainless steel is preferred more than other stainless-steel types due to easiness in welding process. Then, some negative metallurgic changes are taken into consideration in welding of these steels. These are given as; delta ferrite phase, sigma phase, stress-corrosion cracking, chrome-carbide precipitate between grain boundaries at 450–850 °C of Cr–Ni austenitic steels such as 18/8 joined by fusion welding in long waiting time [6].

Stainless steels can be generally welded with all methods of fusion welding and solid state welding. Out of the fusion welding methods, electric arc welding, submerged arc welding, MIG, TIG, Plasma welding, electron beam welding, resistance welding, and laser welding are widely used. In the fusion welding methods for joining the stainless steel, brittle intermetallic compounds phases are produced in the fusion zone, which reduces the strength of the welding joint. However, in the Laser Beam Welding (LBW) joining of stainless steel, because of the reduce of these phases it improves the performance of the stainless steel joint [7, 8, 9, 10, 11, and 12].

Laser welding, using laser beam of high energy density as a heat source, is a highly efficient and precise welding method. It has some excellences, such as high energy density, focalization, deep penetration, high efficiency and strong applicability, and it is widely applied to welding zone requiring the high precision and high quality, including aviation and space technologies, automobile, microelectronics, light industry, medical treatment and nuclear industry. As laser welding is a fast but unbalanced heat-circulation process, larger temperature degrees appear around the weld, therefore the residual stress and deformation of different extent can also appear in the post welding structure. All of these phenomena become important factors, influencing the quality of welding structure and the usable capability. Understanding the heat-process of welding is crucial to analyze the mechanical welding structure and microstructure as well as controlling of welding quality [13, 14, 15, and 16].

In this study, the high heat input in the welding zone and low energy density CO_2 laser welding processes were investigated. A CO_2 continuous wave (CW) laser with a maximum power of 6 kW and a quite large multi-mode power distribution were initially used in a study. CO_2 laser beam welding with a continuous wave has a high energy density and a low heat input process. The result of this is a small heat-affected zone (HAZ), which cools very rapidly with very little distortion, and a high depth-to-width ratio for the fusion zone. The heat flow and the fluid flow in the weld zone can significantly have an effect on the temperature gradients, the cooling rates and the solidification structure. In addition, the fluid flow and the convective heat transfer in the welding zone are known to control the penetration and shape of the fusion zone [17, 18, 19, 20, and 21].

Generally, laser beam welding includes many variables; laser power, welding speed, defocusing distance and type of shielding gas, any of which may have an important effect on heat flow and fluid flow in the welding zone. This in turn will affect the penetration depth, shape and final solidification structure of the fusion zone. Both shape and microstructure of the fusion zone will considerably influence the properties of the welding zone. Many reports [22, 23, and 24] on the shape and solidification structure of the fusion zone of laser beam weldings in relation to different laser parameters are available. However, the effect of all influencing factors of laser welding has not been extensively researched up to now. Many studies are required for understanding the combined effect of laser parameters on the shape and microstructure of the fusion zone. The present investigation is concerned with laser power, welding speed, defocusing distance and type of shielding gas and also their effects on the fusion zone shape and final solidification structure of some stainless steels [25, 26, and 27].

Curcio et al. [28] analyzed the parameters of various materials on laser welding and reported that welding power, welding speed, shielding gas, gas nozzle and the process of focusing were admitted these parameters. Zambon et al. [29] made analyses related the microstructure and tensile strength of AISI 304L super austenitic stainless steel on CO_2 laser welding and demonstrated that in flow resistance and detach tensile a decrease was observed and depending on this decrease, there was also an increase in hardness value because of rapid cooling of the fusion zone during welding. Bertrand et al. [30] studied the Nd YAG laser welding parameters of the stainless steel and reported that laser power and the welding speed were 600-2700 W and 3-10m/min respectively, and the flow speed of the shielding gas was similar to the surface contamination or it underwent a change depending on various surface tensions. El Batahgy [31] investigated the effects of austenitic stainless steels on surface of hardness and fusion zone of laser welding parameters and indicated that penetration increased depending on the increased welding power and welding speed, a significant difference between helium and argon shielding gases was not observed, and mechanical properties (tension, hardness, bending) and fusion zone were not affected by heat input at room temperature. Ghani et al [32] analyzed the microstructural characteristics of low carbon steels on Nd:YAG laser welding and reported that depending on the increased energy input and process speed, the hardness value of the material at welding zone also increased.

In the present paper, dissimilar welded components (AISI 430 ferritic-AISI 304 austenitic stainless steels) were joined by laser beam welding process and the effects of welding speed on the joint integrity was studied.

2. RESEARCH SIGNIFICATION (ÇALIŞMANIN ÖNEMİ)
In this study, the effects of high welding speeds on microstructure and mechanical properties of dissimilar welded components (AISI 430 ferritic stainless steel and AISI 304 austenitic stainless steel) by CO_2 laser beam welding was carried out. The microstructures of the welded joints and the heat affected zones (HAZ) were examined by optical microscopy, SEM, EDS and X-Ray analysis. The tensile strength and microhardness of the welded joints was measured. The result of this study, appropriate joining parameters, joining quality and may occur intermetalic phases of welded samples were determined.

3. EXPERIMENTAL STUDY (DENEYSEL ÇALIŞMA)
3.1. Materials Used in Experiments (Deney Malzemeleri)
3.1.1. AISI 430 Ferritic Stainless Steel
(AISI 430 Ferritik Paslanmaz Çelik)

AISI 430 steels comprise approximately one half of the SAE-AISI type 400 series stainless steels. They are known with their excellent stress corrosion cracking resistance and good resistance to pitting and crevice corrosion in chlorine environments. Welding is known to reduce toughness, ductility and corrosion resistance because of the grain coarsening and carbide precipitations. The grain size gradually increases from the edge of Heat Effected Zone (HAZ) to the fusion boundary. Welding of 400 series usually requires preheat and post-weld heat treatment to minimize stress that can lead to cracking [33].

3.1.2. AISI 304 Austenitic Stainless Steel
(AISI 304 Ostenitik Paslanmaz Çelik)

AISI 304 steels comprise approximately one half of the SAE-AISI type 300 series stainless steels. They are known with their excellent stress corrosion cracking resistance and good resistance to pitting and crevice corrosion in chlorine environments. Austenitic-stainless steel is preferred more than other stainless-steel types due to easiness in welding process. Then, some negative metallurgic changes are taken into consideration in welding of the steels. These are given as; delta ferrite phase, sigma phase, stress-corrosion cracking, chrome-carbide precipitate between grain boundaries at 450–850 °C of Cr-Ni austenitic steels such as 18/8 joined by fusion welding in long waiting time. Welding of 300 series usually requires preheat and post-weld heat treatment to minimize residual stress that can lead to cracking [6 and 34]. The chemical compositions, mechanical and physical properties of both steels were given in Table 1, 2 and 3 respectively.

Table 1. Chemical composition of AISI 430 ferritic and AISI 304
austenitic stainless steels
(Tablo 1. AISI 430 ferritik ve AISI 304 ostenitik paslanmaz çeliklerin
kimyasal bileşimi)

Weight (%) Composition											
Materials	Fe	C	Si	Mn	P	S	Cr	Ni	Cu	Nb	Ti
AISI 430	Balance	0.055	0.045	0.420	0.031	0.008	17.0	–	–	–	–
AISI 304	Balance	0.08	1.00	2.00	0.045	0.03	20.0	10.0	–	–	–

Table 2. Mechanical properties of AISI 430 ferritic and AISI 304
austenitic stainless steels
(Tablo 2. AISI 430 ferritik ve AISI 304 ostenitik paslanmaz çeliklerin
mekanik özellikleri)

Materials	Tensile Strength (MPa)	Yield Strength 0,2% (MPa)	Elongation. (%)	Microhardness (Rockwell B')
AISI 430	517	345	25	170
AISI 304	590	295	55	130-180

Table 3. Physical properties of AISI 430 ferritic and AISI 304 austenitic stainless steels
(Tablo 3.AISI 430 ferritik ve AISI 304 ostenitik paslanmaz çeliklerin fiziksel özellikleri)

Materials	α 10^{-6}	λ W/m $^{\circ}$C	Ω nΩm	E kN/mm^2
AISI 430	13	24	600	225
AISI 304	20	15	700	200
α: Thermal Expansion Coefficient (20-800 $^{\circ}$C)				
λ: Thermal Conductive (20 $^{\circ}$C)				
Ω: Electrical Resistance (20 $^{\circ}$C)				
E: Elastic modulus (20 $^{\circ}$C)				

3.2. Laser Beam Welding (Lazer Işın Kaynağı)

Steel plates to be joined were cut at 60x70x4 mm dimensions. 60 mm width is selected to achieve the standard length of 120 mm tensile test piece. The laser beam welding experiments were carried out under argon and helium shielding gas atmospheres with Trumpf Lazercell 1005 laser welding machine at 2250 W constant heat input and 100-200-300 cm/min welding speeds. Schematic illustration of Laser Beam Welding was given in Figure 1.
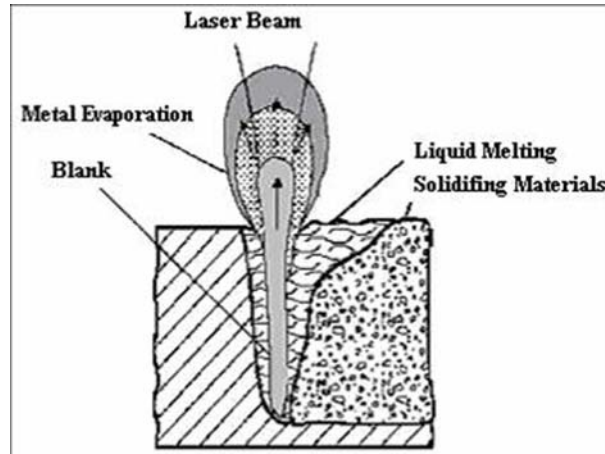

Figure 1. Schematic illustration of laser beam welding process [5]
(Şekil 1. Lazer ışın kaynağının şematik resmi)[5]

3.3. Microstructure Analysis and Microhardness
(Mikroyapı ve Mikrosertlik Analizi)

The Laser Beam Welding was carried out under argon atmosphere, at 2250 W constant heat input and in three (100-200-300 cm/min) different welding speeds. In Figure 2 a-b, 3 a-b and 4 a-b the welding samples are photographed for different heat inputs and welding speeds. The welded specimens were cut in a vertical manner to the welding zone for post evaluations of weld integrity. After the process, the samples were ground to an 80-1200-grit and they were etched by polishing them with 0.3-µm Al_2O_3 diamond paste and aqua regia, respectively.

For microstructural examination, AISI 430 material was etched electrolytically in a solution of 30% HCl + 10% HNO_3 + 30% H_2O solution and AISI 304 material was etched electrolytically in a solution of 50% HNO_3 + 50% H_2O solution. Then the microstructures of the weldings were studied by means of scanning electron microscopy (SEM) equipped with energy depressive spectrometer (EDS). X-ray diffraction analysis was performed to identify the structural phases. Microhardness values were

measured at interface with Leica MHF-10 test apparatus and both sides were analyzed by HV scale under a load of 200 gr (Figure 5). The typical microhardness profile of the welding samples is shown in Figure 6 a-b. Then, from 120 mm length 3 pieces x 20 mm (width) specimens were cut for tensile tests (Figure 7) [35].

4. FINDINGS AND DISCUSSIONS (BULGULAR VE TARTIŞMALAR)
### 4.1. Microstructure (Mikroyapı)

Welding at low travel speed (100 cm/min.) to produce more tapered weld and thus to allow more time for the escape of gases from the molten weld metal also helps to reduce the porosity. At higher travel speeds mainly at 200 and 300 cm/min., slight incomplete penetration and missed seam were traced ending up tensile strength drop at weld interface.

SEM images of welded joints under argon and helium atmospheres at 2250 W constant heat input and at 100-200 and 300 cm/min welding speeds were presented in Figure 2 a-b, 3 a-b and 4 a-b respectively. Grain coarsening was observed at HAZ at both sides of weld interface at AISI 430 ferritic and AISI 304 austenitic stainless steels side at ~200-300μm distance. Naturally, the area of weld (width) and the heat affected zone have decreased while the speeds increased because of less heat input at weld zone. Similar results were achieved at the research studies by Karaaslan et al. and König et al. [33 and 36].

It was determined that in the joint of AISI 430-AISI 304 samples with laser welding at 2250 W heat input, at 100 cm/min welding speed, and under argon atmosphere, the penetration was completed and blanks or porosities in welded area were not observed. It was seen that in joint at 100 cm/min. and under argon shielding gas, the fusion zone was ~1650μm in width, whereas the fusion zone was ~1750μm in width in joint under helium shielding gas. The deep penetration was ~1700μm in depth in joint under argon shielding gas, whereas the deep penetration was ~1800μm in depth in joint under helium shielding gas. It was seen on both sides of the welding seam that a grain hypertrophy occurred both on the AISI 430 side at ~250μm distance, and on the AISI 304 side at ~300μm distance. A homogeneous dispersion with small grains beginning from the zone with coarse grains on both sides appropriate for the original structure of the materials was also observed. The hardness on the welding seam occurred vertically to the main material on the dendritic structure (Figure 2 a-b).
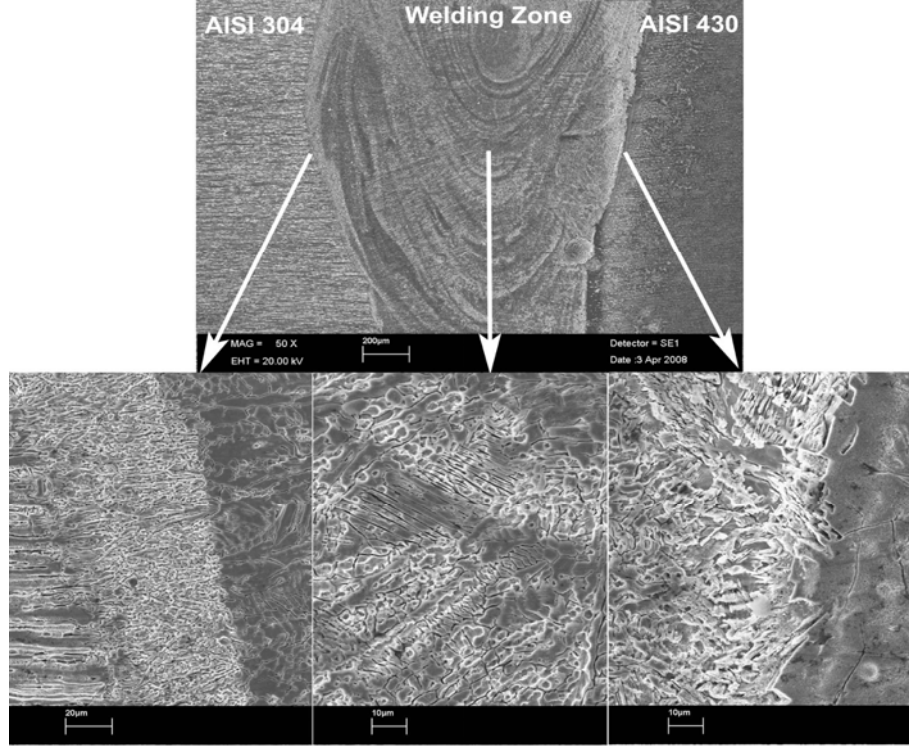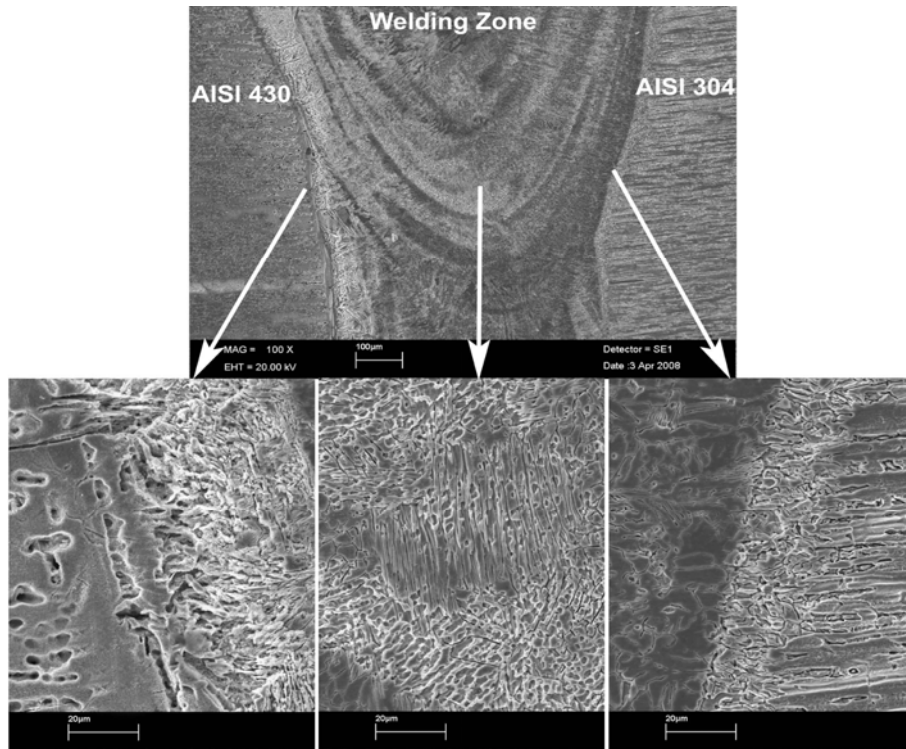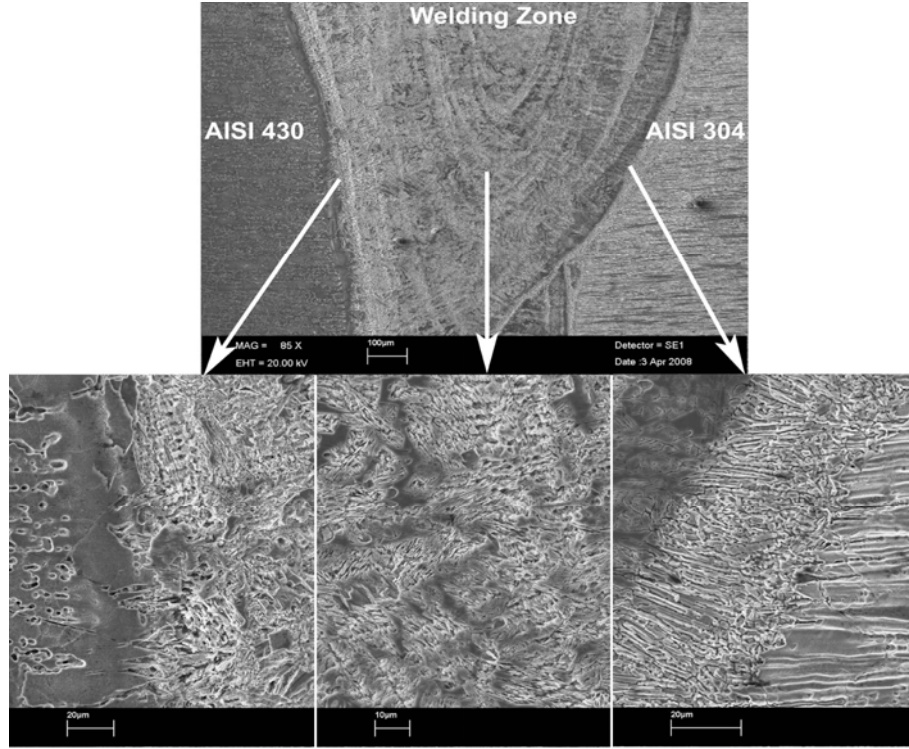
(a)
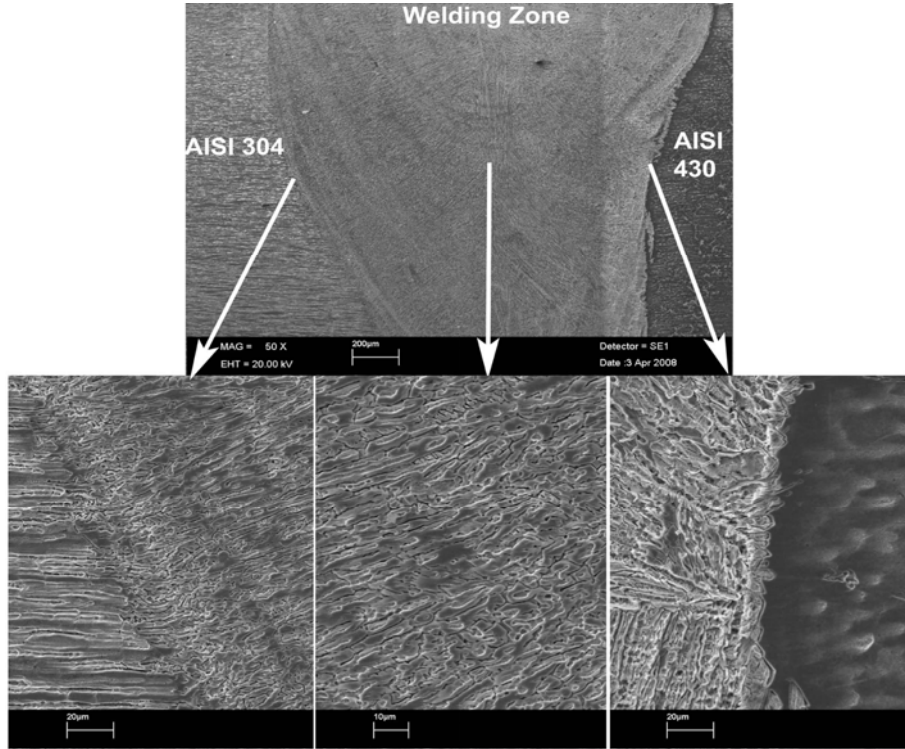
(b)

Figure 2. SEM image of welded sample joined under a) Argon b) Helium
atmosphere at 100 cm/min. welding speed
(Şekil 2. 100 cm/dk. ilerleme hızında a) Argon b) Helyum atmosferi
altında birleştirilen numunenin SEM görüntüsü)

It was determined that in the joint of AISI 430-AISI 1010 samples with laser welding at 200 cm/min welding speed, and under argon shielding gas atmosphere, the penetration was completed and blanks or porosities in the weld were not available. It was seen that in joint at 200 cm/min. and under argon shielding gas, the fusion zone was ~1200µm in width, whereas the fusion zone was ~1250µm in width in joint under helium shielding gas. The deep penetration was ~1600µm in depth in joint under argon shielding gas, whereas the deep penetration was ~1650µm in depth in joint under helium shielding gas. A grain hypertrophy occurred on both sides of the welding zone both on the AISI 1010 side at ~250µm distance, and on the AISI 430 side at ~320µm distance. It was also seen that there was a homogeneous dispersion with small grains beginning from the zone with coarse grains on both sides appropriate for the original structure of the materials. It was observed that the width of the welding zone and HAZ became thinner than that of the joints at 100 cm/min welding speed depending on the increased welding speed. It was determined that at first the grains on the welding zone occurred vertically to the main material beginning from the first zone side where the hardness began and then the first hardened grains did not occur vertically on the dendritic structure in the inner sides of the zone (Figure 3 a-b).
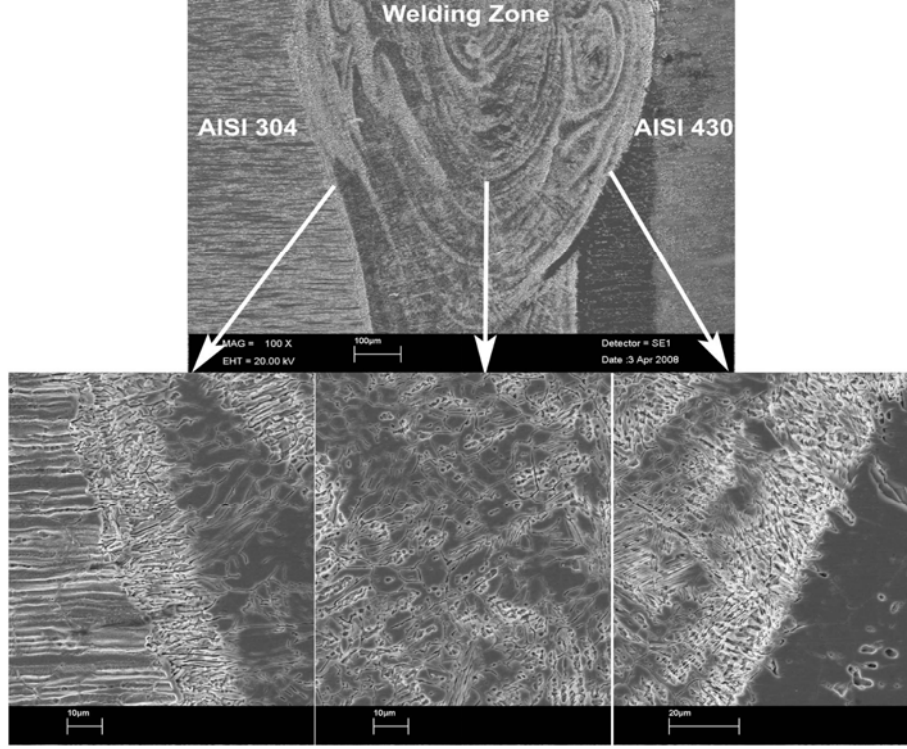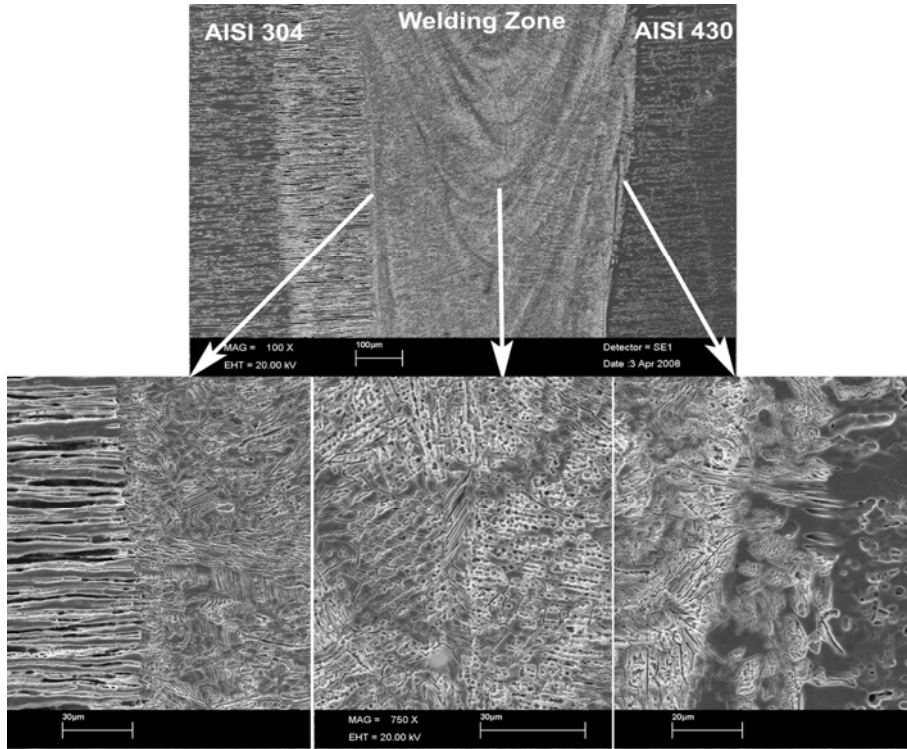

(a)

(b)
Figure 3. SEM image of welded sample joined under a) Argon b) Helium
atmosphere at 200 cm/min. welding speed
(Şekil 3. 200 cm/dk. ilerleme hızında a) Argon b) Helyum atmosferi
altında birleştirilen numunenin SEM görüntüsü)

It was determined that in the joint of AISI 430-AISI 304 samples
with laser welding at 300 cm/min welding speeds, and under argon
atmosphere, the penetration was completed and blanks or porosities in
the weld were not observed. It was seen that in joint at 300 cm/min.
and under argon shielding gas, the fusion zone was ~1050µm in width,
whereas the fusion zone was ~1150µm in width in joint under helium
shielding gas. The deep penetration was ~1500µm in depth in joint
under argon shielding gas, whereas the deep penetration was ~1550µm in
depth in joint under helium shielding gas. It was seen on both sides
of the welding seam that a grain hypertrophy occurred both on the AISI
430 side at ~150µm distance, and on the AISI 304 side at ~200µm
distance. A homogeneous dispersion with small grains beginning from
the zone with coarse grains on both sides appropriate for the original
structure of the materials was also observed (Figure 4 a-b).

(a)

(b)

Figure 4. SEM image of welded sample joined under a) Argon b) Helium
atmosphere at 300 cm/min. welding speed
(Şekil 4. 300 cm/dk. ilerleme hızında a) Argon b) Helyum atmosferi
altında birleştirilen numunenin SEM görüntüsü)

In generally, coefficient of thermal expansion of austenitic stainless steel is greater than ferritic stainless steel. Therefore, all samples on both sides of the welding seam, there was no a specific grain hypertrophy, deformation and crack formation on the main materials. It was also observed that when the seam widths were taken into consideration in terms of shielding gas, the seams performed using helium were much wider than those of the ones performed using argon. Besides, coefficient of thermal conductivity of helium shielding gas is greater than argon gas. Therefore, welding seam is rapid cooling. Moreover, the specific gravity of helium less than air, so the heat generated during welding is to drag along. Depending on it, better and strength welding seam was obtained.

4.2. Microhardness (Mikrosertlik)

The locations of microhardness measurements and microhardness distribution of weld interface were presented in Figure 5 and Figure 6 a-b, respectively.
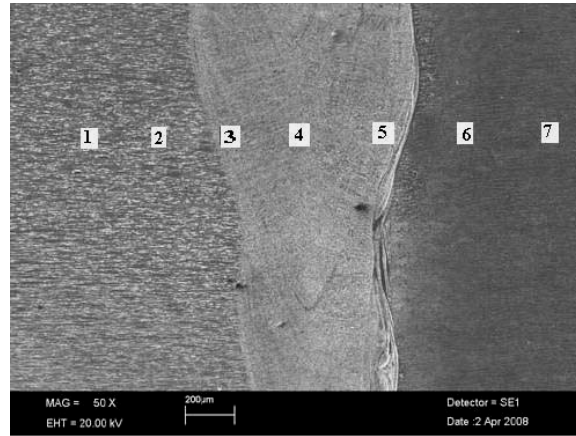

Figure 5. Locations of microhardness measurements of weld interface
(Şekil 5. Kaynaklı numunelerin mikrosertlik ölçüm noktaları)

An average value of hardness was obtained from seven measurements. The typical microhardness profile of the welding samples is shown in Figure 6 a-b.

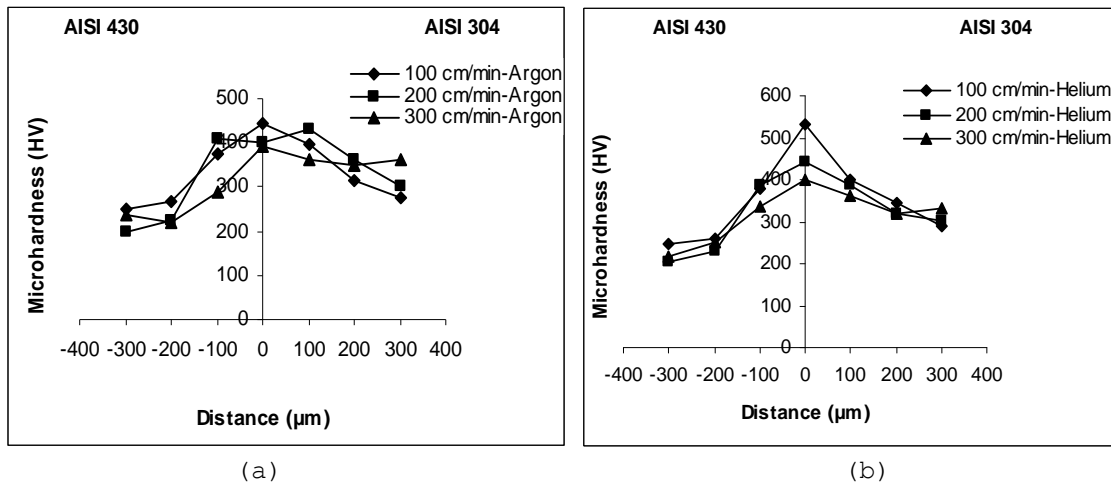(a)   (b)

Figure 6. Microhardness values of weld interfaces a) Argon b) Helium atmosphere
(Şekil 6. Kaynaklı numunelerin mikrosertlik değerleri a) Argon b) Helyum)

170

It is seen that hardness was maximum at the interface for all the joints (about 530 HV) and decreased at different rates toward the main material (about 230-310 HV). Microhardness values can be decreased as long as the welding speed increases. This result shows similarity with Zambon et al. and Ghaini et al. [29 and 32]. This can be explained with the chromium, nickel and carbon diffusion of parent materials at weld interface, thus it has relatively lower hardness. Microhardness values of welding under argon atmosphere were lower than those of welding under helium atmosphere. This can be explained with the fact that helium atmosphere is protecting better than argon atmosphere. Besides, coefficient of thermal conductivity of helium shielding gas is greater than argon gas. Therefore, welding seam is rapid cooling. Moreover, the specific gravity of helium less than air, so the heat generated during welding is to drag along. Depending on it, the rising of microhardness values of welding seam was obtained.

4.3. Tensile Test (Çekme Deneyi)

After Laser Beam Welding, averages of 6 tensile test results on the cold tensile tests were presented in Table 4.

Table 4. Tensile strength of welded samples joined with Laser Beam Welding.
(Tablo 4. Lazer Işın Kaynağı ile birleştirilen numunelerin çekme gerilmeleri).

Samples	Heat input (W)	Welding Speed (cm/min)	Atmosphere	Tensile Strength (MPa)
1		100	Argon	485
2		100	Helium	490
3	2250	200	Argon	460
4		200	Helium	475
5		300	Argon	392
6		300	Helium	451

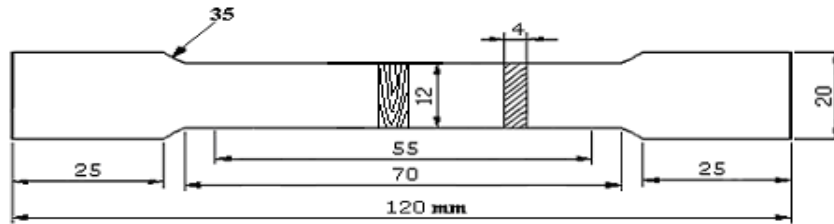Shape and measurement of the tensile specimens were seen in Figure 7.

Figure 7. Shape and measurement of the tensile test specimens [35]
(Şekil 7. Çekme deneyi için kullanılan numunelerin ölçüleri [35])

Plastic deformation detected in the specimens after the welding was not observed. This behavior can also be seen in the micrographs of the fractured surfaces (Figure 8 a-b-c). After welding, it is seen that tensile strength values can be decreased depending on increasing the welding speed, mainly in ductile fracture manner due to the fact that the ferritic stainless steel is a ductile steel (Table 4). Under given conditions (2250 W heat input, 100-200 and 300 cm/min welding speeds) tensile strengths were close to parent material, and slightly decreased at increased welding speeds. This can be explained with the matter of decreased heat input.

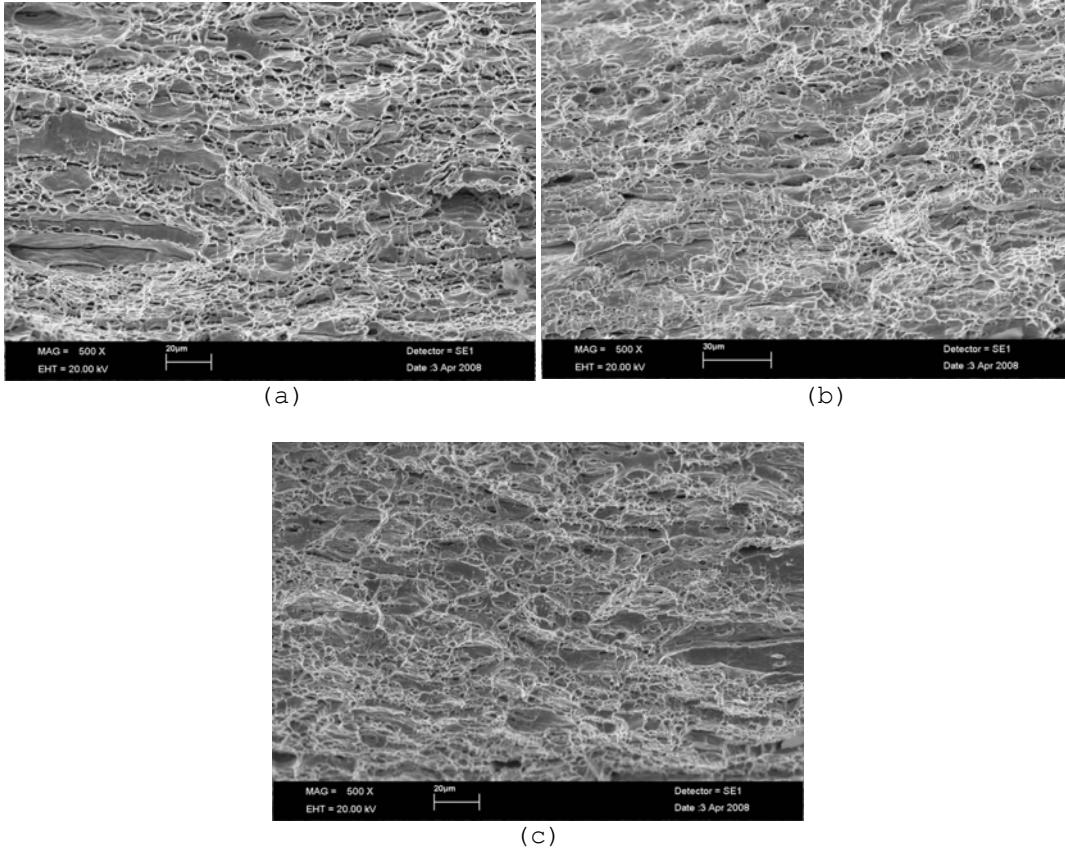(a)   (b)

(c)

Figure 8. Micrographs of the tensile fracture surfaces of the
specimens observed by SEM: a) 100 b) 200 c) 300 cm/min
(Şekil 8. Numunelerinin çekme sonrası oluşan a) 100 b) 200 c) 300
cm/dk kırık yüzeylerinin SEM görüntüleri)

The lowest value according to tensile strength values, under
argon atmosphere was obtained in the joints performed at 300 cm/min
welding speed (392 MPa) and the highest value was obtained in the
joints performed, under helium atmosphere at 100 cm/min welding speed
can be seen in Table 4 (490 MPa). Tensile strength values of welding
performed under argon atmosphere were lower than those of welding
performed under helium atmosphere. The fact that helium atmosphere is
protecting better than argon atmosphere can help to explain this. It
can be suggested that helium rises when it taking away a little heat
from the atmosphere. Depending on it, better and strength welding seam
was obtained (Table 4).

4.4. X-Ray diffraction and EDS Analysis
(X-Ray ve EDS Analizleri)
In the EDS analysis, as well as C, Cr and Ni elements, no
chromium-carbide, delta ferrite phase and sigma phase like
intermetalic phases determined in the welding interface were detected.
In the 200 µm distance, from AISI 304 austenitic stainless steel to
AISI 430 ferritic stainless steel 16% chromium, 1,5% carbon and 1%
nickel diffusion, the equal distance occurred from AISI 430 steel to
AISI 304 steel chromium and carbon diffusion. Because, carbon is an
interstitial element and stainless steel side will diffuse more
easily. It is seen that chromium-nickel diffusion can be decreased by
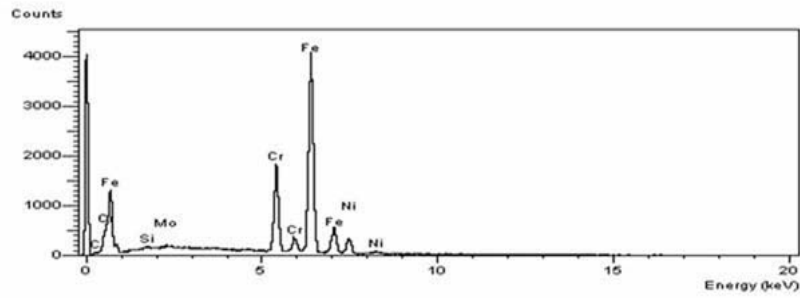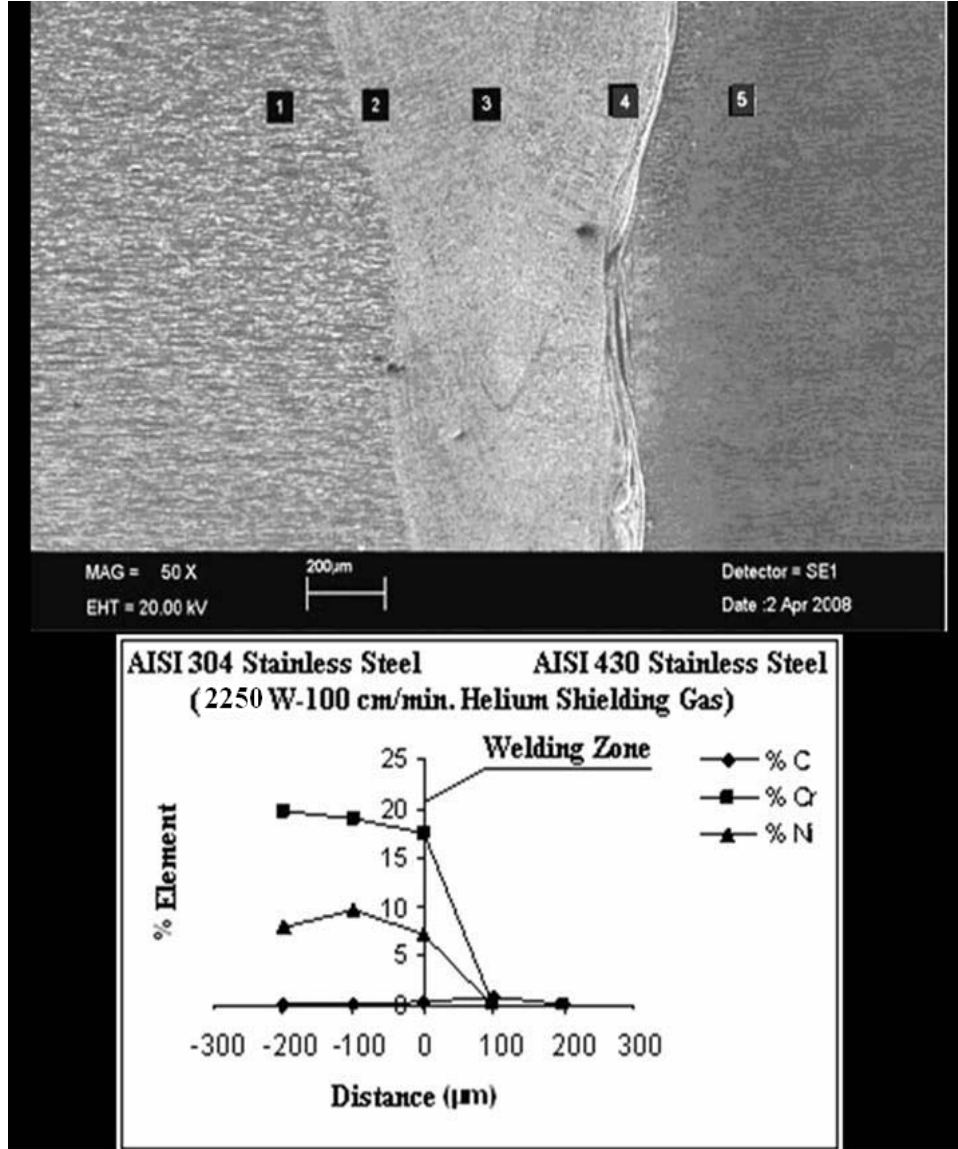increasing the welding speed (Figure 9).

Figure 9. EDS Analysis of AISI 430/304 (2500 W-100 cm/min.-Helium)
sample
(Şekil 9. AISI 430/304 numune çiftinin (2500 W-100 cm/dk.-Helium) EDS
analizi)

In the X-Ray analysis, like Fe, Ni-Cr-Fe, Fe-Cr-Co-Ni-Mo-W and $Cr_2Fe_{6.7}Mo_{0.1}Ni_{1.3}Si_{0.3}$ phases were determined (Figure 10).

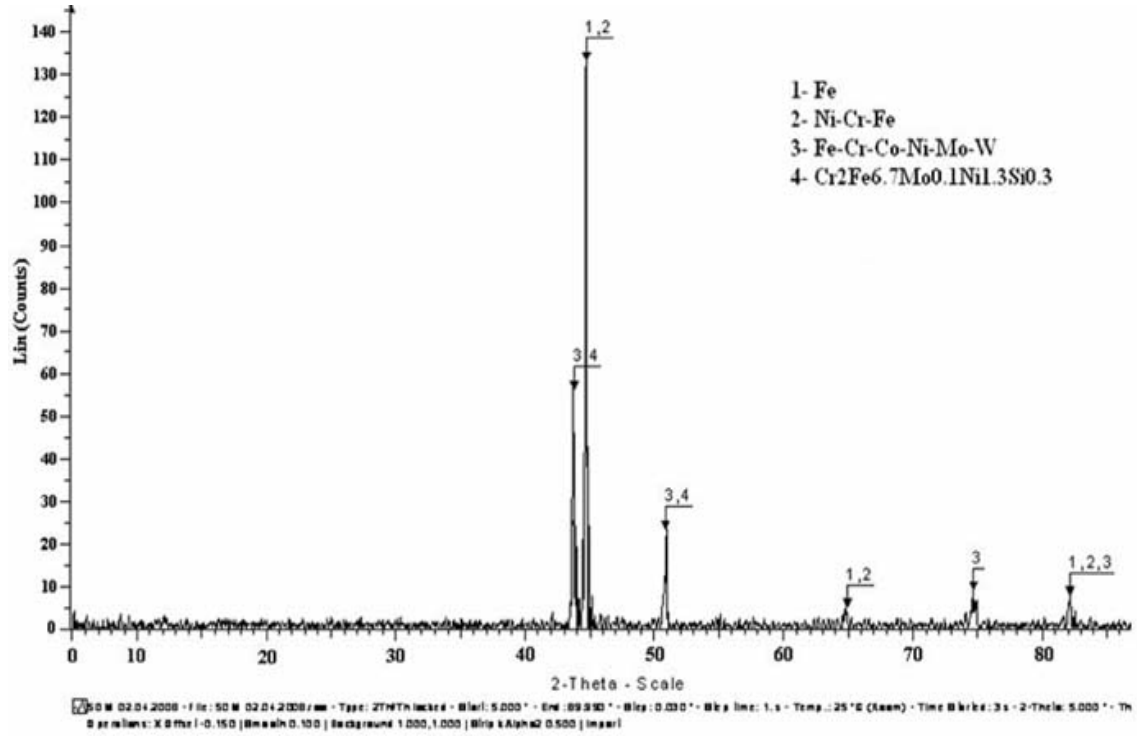Figure 10. X-Ray Analysis of AISI 430/304 (2500-100-Helium) sample
(Şekil 10. AISI 430/304 numune çiftinin (2500 W-100 cm/dk.-Helium)
X-Ray analizi)

5. CONCLUSIONS (SONUÇLAR)

In this study, microstructural characteristic of dissimilar welded components (AISI 430 ferritic-AISI 304 austenitic stainless steels) by CO_2 Laser Beam Welding (LBW) was analyzed. The obtained results were as following;

- AISI 430 ferritic stainless steel can be joined with AISI 304 austenitic stainless steel by laser welding process using argon atmosphere, 2250 heat input, 100-200 and 300 cm/min welding speeds.

- It was seen that hardness determined maximum ~530 HV at the interface at 2250 W heat input and at 100-200-300 cm/min. welding speeds joints and then the hardness decreased at different rates toward the main material's hardness value (~230-310 HV). Microhardness values decreased due to the increasing welding speed. Microhardness values of welding under argon atmosphere were lower than those of welding under helium atmosphere.

- At tensile strength tests, fractures were observed closed to AISI 430 side. After welding, it was seen that tensile strength values tensile strength values decreased due to the increasing the welding speed. This is because of the fact that ferritic stainless steel is a ductile steel. The lowest value according to tensile strength values, under argon atmosphere was obtained in the joints performed at 300 cm/min welding speed (392 MPa); and the highest value was obtained in the joints performed, under helium atmosphere at 100 cm/min welding speed (490 MPa).

174

It was also observed that the results of tensile strength test of joints performed at 200 cm/min. welding speed had values between 460 and 475 MPa. Economically, high tensile strength with low heat input is demanded. These circumstances were obtained at 2250 W heat input, 100 cm/min. welding speed and helium shielding gas. (Table 4 (490 MPa).

- It was determined that in joint of AISI 430-AISI 304 samples with laser welding at 2250 W constant heat input, at 100-200 and 300 cm/min welding speeds, and under argon and helium atmospheres, the fusion zone was on average ~1050-1750 μm in width, the deep penetration was on average ~1500-1800 μm in depth. Coefficient of thermal expansion of austenitic stainless steel is greater than ferritic stainless steel. Therefore, on both sides of the welding seam, there was no a specific grain hypertrophy, deformation and crack formation on the main materials.

- The best properties in terms of microstructure, microhardness and tensile test were observed at the specimen bonded at 2250 W heat input, at 100 cm/min. welding speed and helium shielding gas. It was also observed that when the seam widths were taken into account consideration in terms of shielding gas, the seams performed using helium were much wider than those of the ones performed using argon.

- In the EDS analysis, in the 200μm distance, from AISI 304 austenitic stainless steel to AISI 430 ferritic stainless steel 16% chromium, 1,5% carbon and 1% nickel diffusion, the equal distance occurred from AISI 430 steel to AISI 304 steel chromium and carbon diffusion. Because, Carbon is an interstitial element and stainless steel side will diffuse more easily. It is seen that chromium-nickel diffusion can be decreased by increasing the welding speed.

- In the X-Ray analysis, like Fe, Ni-Cr-Fe, Fe-Cr-Co-Ni-Mo-W and $Cr_2Fe_{6.7}Mo_{0.1}Ni_{1.3}Si_{0.3}$ phases were determined. It wasn't observed intermetalic phase like $Cr_{23}C_6$ (Chromium Carbide).

REFERENCES (KAYNAKLAR)
1. Yi-Chun L. and Ming-Huei Y., (2007). Effects of Laser Beam Energy and Incident Angle on the Pulse Laser Welding of Stainless Steel Thin Sheet, Journal of Materials Processing Technology, 190, 102–108.
2. Taskin, M., Ozan, S., and Kolukisa, S., (2006). The Effect of the Process Temperature on the Bondability in Diffusion Bonding of AISI 430 with Nodular Cast Iron, Practical Metallography, 43(6), 293-305.
3. Ozan, S., Taskin, M. and Kolukisa, S., (2006). The Effect of the Process Temperature on the Bondability in Transient Liquid Phase (TLP) Diffusion Bonding of AISI 430 Ferritic Stainless Steel with Nodular(Spheroid) Cast Iron Using A Copper Interlayer, Practical Metallography, 43(11), 575-585.
4. Moustafa, I. M., Moustafa, M. A. and Nofal, A.A., (2000). Carbide Formation Mechanism During Solidification and Annealing of 17% Cr-Ferritic Steel, Materials Letters, 42(6), 371-379.
5. Taskin, M., Caligulu, U., and Kolukisa S., (2009). The Effect of Welding Speed on the Laser Welding of AISI 430 Ferritic

Stainless-AISI 1010 Low-Carbon Steel, Practical Metallography, 46(11), 598-608.

6. Sahin, M., (2007). Evaluation of the joint interface properties of austenitic-stainless steels (AISI 304) joined by friction welding, Materials and Design, 28, 2244-2250.

7. Aran, A. and Temel, M. A., (2004). Paslanmaz Çeliklerin Üretimi, Kullanımı, Standartları, Sarıtaş Teknik Yayınları No:1, 2. Baskı, 54-65.

8. Hussain, P. and Isnin, A., (2001). Joining of Austenitic Stainless Steel and Ferritic Stainless Steel to Sialon, Journal of Materials Processing Technology, 113, 222-227.

9. Chih-Chun Hsieh et al., (2008). Precipitation and Strengthening Behavior of Massive δ-Ferrite in Dissimilar Stainless Steels during Massive Phase Transformation, Materials Science and Engineering A, 477, 328-333.

10. Earle W. and Rockwell R.J., (2001). Safety Fundamentals for Today's Industrial Lasers, as Laser Use Increases, so does the Importance of Safety, The Fabricator.

11. Yilbas, B.S., Sami, M., Nickel, J., Coban, A., and Said, S.A.M., (1998). Introduction into the Electron Beam Welding of Austenitic 321-Type Stainless Steel, Journal of Materials Processing Technology, 82, 13-20.

12. Yilbas, B.S., Shuja, S.Z., Arif, A., and Gondal M.A., (2003). Laser-Shock Processing of Steel, Journal of Materials Processing Technology, 135, 6-17.

13. Yilbas, B.S., (1997). Parametric Study to Improve Laser Hole Drilling Process, Journal of Materials Processing Technology, 70, 264-273.

14. Bayraktar, E., Kaplan, D., and Yilbas, B.S., (2008). Comparative Study: Mechanical and Metallurgical Aspects of Tailored Welded Blanks (TWBs), Journal of Materials Processing Technology, 204, 440-450.

15. Han GuoMing, Zhao Jian and Li JianQang, (2007). Dynamic Simulation of the Temperature Feld of Stainless Steel Laser Welding, Materials and Design, 28, 240-245.

16. Benyounis, K.Y., Olabi, A.G., and Hashmi, M.S.J., (2005). Optimizing the Laser-Welded Butt Joints of Medium Carbon Steel Using RSM, Journal of Materials Processing Technology, 164-165, 986-989.

17. Behler et al., (1997). Laser Beam Eelding of Low Weight Materials and Structures, Materials and Design, 18(4), 261-267.

18. Zacharia T. et al., (1989). Metall. Trans., 20 A, 1125.

19. Anawa E.M. and Olabi A.G., (2008). Control of Welding Residual Stress for Dissimilar Laser Welded Materials, Journal of Materials Processing Technology, 204, 22-33.

20. Benyounis, K.Y., Olabi, A.G., and Hashmi, M.S.J., (2005). Effect of Laser Welding Parameters on the Heat İnput and Weld-Bead Profile, Journal of Materials Processing Technology, 164-165, 978-985.

21. Alabeedi, K.F., Abboud ,J.H. and. Benyounis, K.Y., (2009). Microstructure and Erosion Resistance Enhancement of Nodular Cast Iron by Laser Melting, Wear, 266, 925-933.

22. Suutala, N., (1983). Metal. Trans., 14 A, 191.

23. David, S.A. and Vitek, J.M., (1981). Laser in Metallurgy, Conference Proceedings of the Metallurgical Society of AIME, 147.

24. Arata, J., Matsuda, F., and Katayama, S., (1976). Trans., JWRI 5, 35.

25. Mazumder, J., (1993). Laser Beam Welding, ASM Handbook, 6, 262-269.
26. Abbott, D.H. and Albright, C.E., (1994). CO_2 Shielding Gas Effects in Laser Welding Mild Steel, Journal of Laser Applications, 6, 69-80.
27. Johnson, D., Penn, W., and Bushik, S., (2008). Application Experiences with Laser Beam Welding, Alabama Laser, 1-5.
28. Curcio et al., (2006). On the Welding of Different Materials by Diode Laser, Journal of Materials Processing Technology, 175, 83-89.
29. Zambon, A., Ferro, P., and Bonollo, F., (2006). Microstructural, Compositional and Residual Stress Evaluation of CO_2 Laser Welded Superaustenitic AISI 904L Stainless Steel, Materials Science and Engineering A, 424, 117-127.
30. Bertrand, P., Smurov, I., and Grevey, D., (2000). Application of Near Infrared Pyrometry for Continuous Nd: YAG Laser Welding of Stainless Steel, Applied Surface Science, 168, 182-185.
31. El-Batahgy A.M., (1997). Effect of Laser Welding Parameters on Fusion Zone Shape and Solidification Structure of Austenitic Stainless Steels, Materials Letters, 32, 155-163.
32. Ghaini et al., (2007). Weld Metal Microstructural Characteristics in Pulsed Nd: YAG Laser Welding, Scripta Materialia, 56, 955-958.
33. Karaaslan, A., Sonmez, N., and Topuz, A., (1998). The Investigation on Non-alloyed Construction Steel Weldability with Laser, 2. International Welding Technology Conference.
34. Sahin, M. and Akata H.E., (2004). An experimental study on friction welding of medium carbon and austenitic stainless steel components, Indust. Lubricat. Tribol., 56(2), 122-129.
35. Kayali, E.S., Ensari, C., and Dikec, F., (1983). Metalik Malzemelerin Mekanik Deneyleri, ITU Library, 22-31.
36. Konig, R. and Otmanboluk, N., (1998). Metal Cutting and Welding Process with CO_2 and Nd-YAG Laser, 2. International Welding Technology Conference.